SECTOR ENERGÍA Y MINAS
INGEMMET
INSTITUTO GEOLÓGICO, MINERO Y METALÚRGICO

Chemical and isotopic composition of hot spring waters in the Tacna region, Southern Peru

Vicentina Cruz Pauccara[1]

[1] Instituto Geológico Minero y Metalúrgico, Av. Canadá Nº 1470, San Borja Lima 41, Perú, Apartado 889 (vcruz@ingemmet.gob.pe, vcruz24@hotmail.com).

Keywords: geothermal areas, Tacna, Quaternary volcanism, geothermometry, southern Peru.

ABSTRACT

The Tacna region hosts the most promising geothermal zones of Southern Peru, comprising five main geothermal areas: Tutupaca, Calientes, Borateras, Ancocollo and Chungara- Kallapuma located along the Quaternary volcanic chain at a height of 4000-4400 m on the Cordillera de los Andes. In these areas, we studied the chemical and isotopic composition of thermal waters. The geochemical characterization of the thermal discharges shows, the presence of two different types of thermal spring in Tacna region Na^+-Cl^- and Ca^{2+}-SO_4^{2-} waters. The Na^+-Cl^- springs, controlled by magma degassing and by water-rock interaction processes. Ca^{2+}-SO_4^{2-} waters are supply by shallow meteoric water heated by ascending gases and are characterized by a low pH. Chloride water is rich in B, As and SiO_2, suggesting interactions of deep-originated fluids with meteoric waters at shallow depth. The relatively high boron concentrations in the geothermal waters may be due to deep circulation paths that interacted with different lithologies at depth associated to sedimentary rocks. The isotopic composition δ^2H and $\delta^{18}O$ indicates that the geothermal reservoir waters originate from a mixture of meteoric and magmatic water, with temperatures exceeding 200°C estimated by geothermometry, indicate that geothermal areas can be regarded as the most promising areas and deserve more detailed geological and geophysical investigations for determination the geothermal potential.

1. Introducción

Tacna region is located in southern Peru; it extends from the Pacific Ocean rising towards the summit of the Western Cordillera of Andes. This region is limited to the north with Puno, to the NE with Moquegua, to the E with Bolivia, and with Chile to the SE (Fig. 1).

The most promising geothermal zones of the country are located in Tacna region due to the presence of the Quaternary volcanic arc of southern Peru named "Eje Volcanico Sur" (Vargas et al., 2010), which is part of the continental volcanic arc of the Central Volcanic Zone (CVZ) located in the Cordillera Occidental. De Silva and Francis (1991) subdivide the CVZ in two zones based on the orientation of the volcanic arc: the NW-SE-trending chain of volcanoes in southern Perú and the N-S oriented chain in northern Chile. Presence of numerous hot springs, fumaroles, and geysers associated to these volcanic chain shows that the heat is transferred continuously to the surface by conduction and convection; the latter process involves the discharge of geothermal fluids from numerous geothermal fields.

Evaluation of Tacna region geothermal potential started in the 70´s where most of the studies were undertaken by government institutions, with some technical assistance from countries that have developed geothermal activities. However, like many countries, in Peru with the objective of satisfying energy demand and diversify energy sources with clean energy, the feasibility of using high temperature geothermal fields is being investigated. Numerous studies have been developed to determine the origin of geothermal water and the hydrogeochemical processes taking place in these waters. These studies have included the determination of the chemical–physical conditions acting on the fluid reservoirs to provide information for the evaluation of their geothermal potential (Tassi et al., 2010; Sepulveda et al., 2004); to define the structural elements of geothermal systems (Favara et al., 2001), and to delineate the role of magmatic sources in providing water and elements compared to the meteoric source and water-rock interaction (Cortecci et al., 2005). A geochemical survey for developing a conceptual model of the hydrothermal system has also been carried out (Riogilang et al., 2013).

This paper reports studies carried out in five geothermal areas: Calientes, Borateras, Tutupaca, Ancocollo and Kallapuma-Chungara, located along the Quaternary volcanic

chain in southern Peru, where geothermal manifestations are evidenced by the prevalence of geothermal waters.

The purpose of the present study is to characterize the physic-chemical conditions and the circulation depth along with the understanding of the mixing processes between meteoric and magmatic water by means of hydrochemical and isotopic methods.

This research will contribute to the evaluation of the energetic potential of geothermal resources, and contribute to the sustainable utilization and protection of thermal waters in the Tacna region.

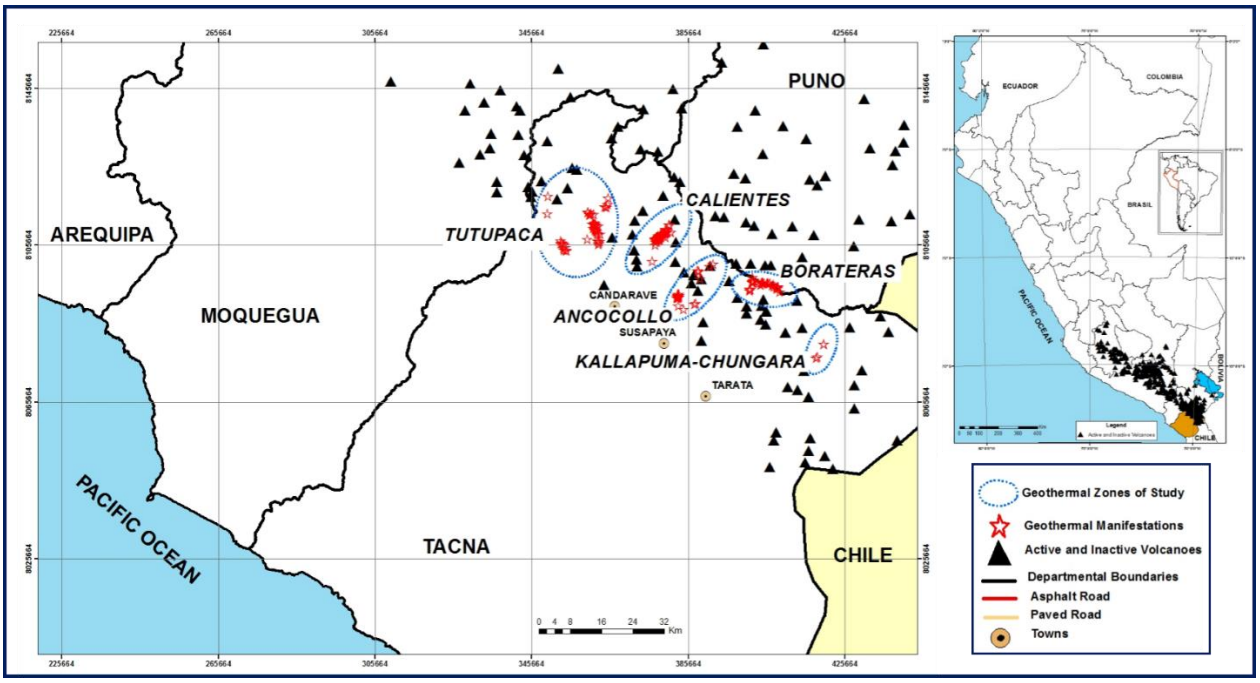

Fig. 1. Location of the Tutupaca, Calientes, Ancocollo and Kallapuma-Chungara geothermal areas in the Tacna region, southern Perú.

2. Contexto geológico

According to the regional setting, the geological units in the area where the five promising geothermal areas are located are: Yura Group sedimentary rocks, intrusive of the Toquepala arc and volcanic rocks of the Paleogene and Neogene (Fig. 2).

The Yura Group is composed of sedimentary rocks exposed in a limited way in the foothills of the western cordillera mountains, in the Jaruma River and north of Tarata, where the Cachíos, Labra and Gramadal Formations of the Upper Jurassic and Hualhuani of Lower Cretaceous have been recognized. The oldest unit outcropping is the Cachios Formation of the Caloviana age (Benavides, 1962), and consists of black shales, sometimes slaty, some thin bars of sandstone found in slipped packages, in shape of olistolites with presence of fossil bivalves (Vicente et al. 1979; Carlotto, 2009).

The Toquepala intrusive outcrops in the southwestern part of Candarave and consists of Paleocene granodiorites. On the other hand, north of Tarata granodiorite outcrops have been dated at 44 ± 4.3 My (Clark, 1990).

The volcanic rocks of the Paleogene-Neogene are composed of the following units: Tacaza, Huaylillas and Barroso. The Tacaza Group (24-30 My) is represented by ignimbrites and sedimentary-volcano deposits seen on the western edge of the western cordillera. The Huaylillas Formation (10-24 My) is also located on the western edge of the western cordillera covering a large area of the southwestern part of the study area. In addition, Barroso Group (3-10 Ma) is widely distributed in much of the studied geothermal areas, mainly in the cordillera zone, as eroded volcanic structures that protrude from the plateau (Cereceda, 2012).

Finally, current volcanic deposits limited in extent are also present in the area, consisting of active stratovolcanoes including Tutupaca and Yucamane. These volcanoes are composed of lava flows, pyroclastic flows, tephra and subvolcanic domes (Fig. 2). In the study area, Tacna region has recorded the presence of more than 64 volcanic centers, among which stand out for their recent activity, Tutupaca, Yucamane, Purupurune and Casiri volcanoes (Fig. 4). These volcanoes have a NW-SE and NE-SW regional structural control (Steinmüler, K. & Zavala, B., 1997).

3. Tectonic setting and geothermal resources

The western coast of South America is the only major active margin along which an oceanic plate (Nazca Plate) underthrusts a continent (South America). Numerous studies based on seismicity and geological data have shown that the Andean margin can be subdivided into five tectonic segments between latitudes 0˚S and 45˚S (e.g., Stauder, 1975; Barazangi and Isacks 1976; Jordan et al., 1983). These segments alternate between modes of normal and flat subduction. Zones of normal subduction (Fig.3) are associated with an active volcanic front (southern Ecuador, southern Peru and northern Chile, and southern Chile) (Norabuena, 1992).

The zones of normal subduction are characterized by high temperatures due to the accumulation of magmatic bodies (Babeyko et al., 2002) capable of generating numerous volcanic eruptions (Baker, 1981; Lahsen, 1982; de Silva, 1989; Chmielowsky et al., 1999). Surface outcrops of young volcanic rocks show an abrupt increase in southern Peru, coincident with the start of the Altiplano. Figure 3 shows the distribution of active volcanoes and volcanic centers younger than Miocene. However, in the entire Neogene period, the volcanic centers have been distributed almost all over the Altiplano. A wide distribution of volcanism is also consistent with high heat flow observed not only near the Western Cordillera but in most part of the Altiplano. This implies that a much wider region has been under the influence of volcanic activity, and a considerable amount of magmatic material that was due supplied to the crust beneath the Western Cordillera as well as the Altiplano (Kono et al., 1989). Kono et al. (1989) suggests that the volcanic activity in the Andes of southern Peru is perhaps distributed over a wide geographical extent covering most of the Altiplano, and that the Altiplano corresponds roughly to the area of magma generation associated with the subduction of the Nazca plate beneath the South American plate.

The volcanic arc in southern Peru is part of the Western Cordillera, whose highest point is 6000 m, this arc is located at approximately 280 km from the ocean trench and about 115 km from the plane of Benioff-Wadati (Barazangi & Isacks, 1976). This volcanic chain is represented by stratovolcanoes with a central crater and dome, plus small monogenetic cinder cones associated with lava flows <5000 BP (Delacour et al., 2007; De Silva and Francis, 1991).

Therefore, the geothermal resources in Tacna region are mainly related to the presence of volcanic activity (Quaternary volcanism). The high temperatures registered in the thermal manifestations are related to the presence of heat sources (magma chambers). All these volcanic structures are strongly fractured controlling the recharge, circulation and discharge of geothermal fluids, whether in deep or subsurface areas, and observed at surface as hot springs, geysers and fumaroles (Steinmüler, K. & Zavala, B., 1997; Cruz et al, 2013).

.

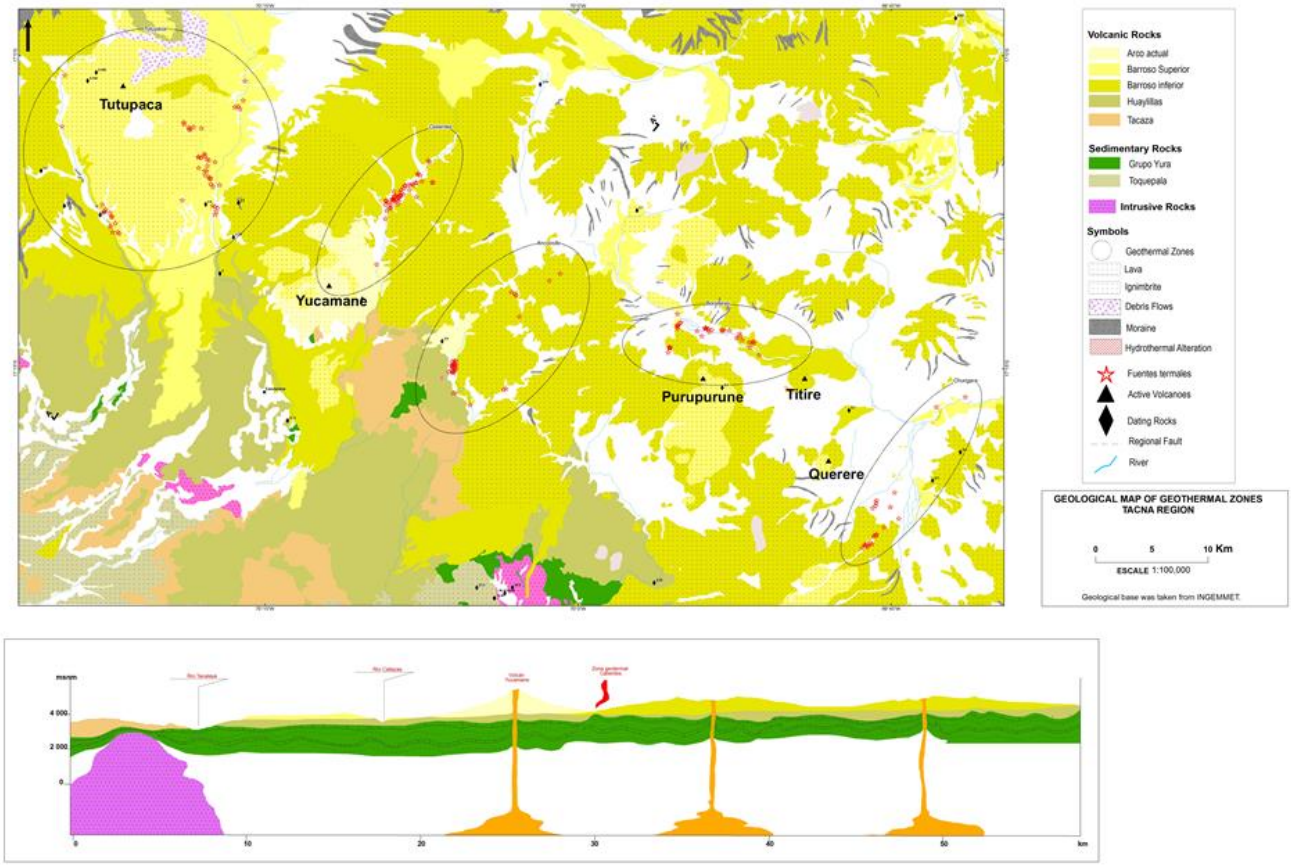

Fig. 2. Geological map of the Tutupaca, Calientes, Ancocollo and Kallapuma-Chungara geothermal areas (Cruz et al, 2013).

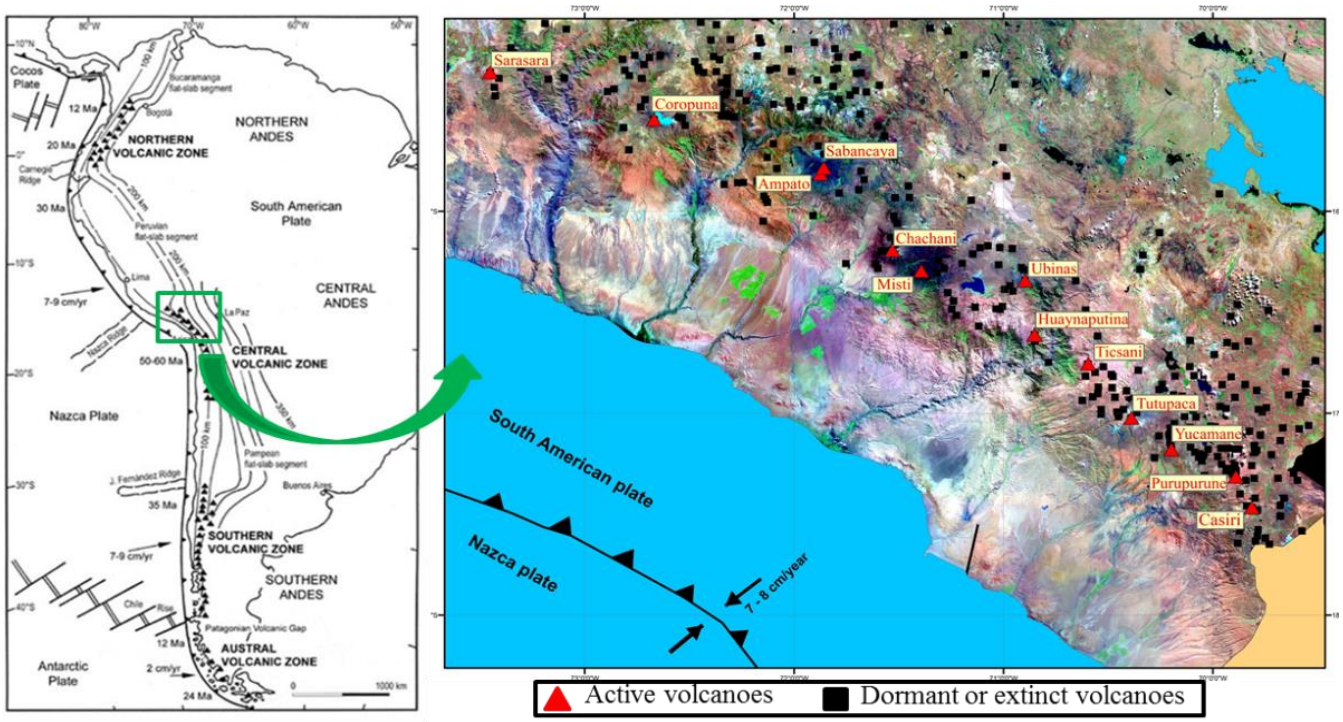

Fig. 3. Schematic map of South America and the pacific oceanic plates and Central Volcanic Zone in southern Perú (Ramos and Alemán, 2000; de Silva and Francis, 1991).

3.1 Tutupaca

The Tutupaca geothermal zone is located in Tacna region at an altitude between 4000 and 4500 m a.s.l. In this geothermal area, the presence of the Tutupaca volcanic complex is evidenced. The Tutupaca volcanic complex (17 ° 01 'S, 70 ° 21' W) is located on the southeastern part of the Peruvian volcanic arc. This volcano is considered active, because several eruptions occurred during the historical period. Volcanic activity reports have been compiled by the "Global Volcanism Program" (Siebert et al., 2010). Also, Zamacola and Jaúregui (1804) and Valdivia (1847) clearly indicate that Tutupaca has had at least two eruptive periods in 1789 and 1802 (Manrique et al., 2013).

In Tutupaca, 50 geothermal manifestations of various types were recorded: hot springs, mud pools, fumaroles and steam sources. These arise in four sectors: Callazas River, Pampa Turun Turun, Tacalaya River and the sulphur area (Azufre Grande and Azufre Chico) (Fig. 4a). This area is surrounded by two main rivers, Callazas to the east, and Tacalaya to the west, both controlled by structural lineaments.

In the Tutupaca geothermal area, volcanic rocks corresponding to Tutupaca active volcano are observed. This volcano is situated over a substrate composed of Huaylillas Formation ignimbrites, that has been dated between 12-24 My. Furthermore, volcanic rocks of the Upper Cretaceous to Pliocene, like the Toquepala Group, Barroso Group and Sencca Formation (Manrique et al., 2013) were identified near the volcano. Besides, this volcano consists of an alternate sequence of pumice pyroclastic flows and ash with massive blocks, overlaid by an important sequence of andesitic and trachytic lavas flows, and finally a trachyandesitic debris flow tuff with abundant hornblende crystals containing, biotite, pyroxene and quartz on the top (De la Cruz and De la Cruz, 2001).

Beneath these rocks and in the southern part of the volcano the Huaylillas Formation (Miocene) outcrops: it consists of pyroclastic flows, rhyolitic tuffs and andesite blocks. In the Tutupaca area, there are deposits of whitish precipitates, specifically in the Turun Turun and Tacalaya sectors. Precipitates from hot springs are composed of amorphous silica sinter, altered zones are found preferably in intersection zones of different tectonic structures and around volcanic structures, also the central zone of the volcano Tutupaca has hydrothermal altered zones (De la Cruz and De la Cruz, 2001).

In the Tutupaca geothermal area, the structural context is characterized mainly by regional NW-SE guidelines and local NNW-SSE and NNE-SSW faults. The stratigraphy, geological structures and the distribution of surface thermal manifestations, indicate that geothermal fluids are controlled by permeable zones associated with faults (Fig. 4a). Furthermore, the identification of the Tutupaca fault with NE-SW direction indicates that a large fracturing seems to control fissure volcanism (Torres, et. al. 1997).

The local NNW-SSE structures seem to determine the upwelling of geothermal manifestations, as in the case of the streams Azufre Grande and Azufre Chico. De la Cruz (De la Cruz and De la Cruz, 2001) describes a large geological lineament, which determines the course of the Tacalaya River.

3.2 Calientes

Calientes geothermal area is located east of Yucamani active volcano in Candarave's province, Tacna region at an altitude of 4400 meters. This valley is narrow in the northern part (0.8 km) and broader in the south part, with approximately 2 km along Calientes River. Thermal discharges occur in an area of approximately 14 km^2, with manifestations of hot springs, pools with bubbling gas and geysers with low flow and pressure.

Calientes is characterized by the presence of several volcanic systems and tectonic structures with a direction mainly NE-SW (Fig. 4b). In the western part of the valley, we can see the volcanic complex "Yucamane–Calientes–Yucamane Chico", constituted principally by lava flows, domes of lava and some remnants of pyroclastic flows. Of all these volcanoes, Yucamane the most active, whereas Calientes and Yucamane Chico volcanoes, located to the northern part had activity possibly before the Pleistocene. The hot spring in Calientes is located in a fluvial valley surrounded by a volcanic chain of Pleistocenic age having an anti-Andean direction, NE – SW, which is a typical morphology of the southern Andes of Perú (Cruz et al., 2010).

Yucamane volcano has mainly produced andesitic lava flows, block and ashes pyroclastic flows associated with lava domes. The stratigraphy indicates several volcanic events.

Holocenic deposits correspond to alluvial, colluvial and swamp; are shape by accumulations of reworked gravels, sands and silt. These deposits are mainly refilling the current riverbeds of streams and rivers. In the middle and top part of the Calientes Valley, we have a big sinter deposit, formed by carbonate and silica precipitation. The swamps are located mainly in the saturated sediments of streams.

In the southern part of Yucamane volcano, small outcrops of quartz sandstone from Hualhuani Formation, Yura Group are present. Limestones from Gramadal Formation from Yura group outcrop south of Calientes geothermal field. This information indicates that sedimentary rocks constitute the bedrock on which diverse Neogene volcanic episodes have occurred.

A regional geological structure characterized by a structural NW-SE fault and parallel to the Andean and volcanic chain direction is present in Calientes geothermal zone. The volcanoes around Calientes are aligned in a direction NE-SW, indicating the presence of a fault along this direction. The structural system is summarized as: structures with NE-SW (well identified) tendency going along Calientes River, where surge to numerous hot springs in the same direction. Therefore, this system of lineaments seems to be the fault of the system "Fc-1". In addition to the described system, faults have been identified with N-S "Fc-2" direction determining the course of Calientes River in the southern part of the valley; along these structures, geothermal manifestations are not present. Likewise, the analysis of satellite images indicates the presence of a fault with NNW-SSE direction (Fc-3) (Fig. 4b) (Vargas, et al., 2012, Cruz et al., 2010).

3.3 Ancocollo

Ancocollo geothermal area is located southeast of the active volcano Yucamani, 9 km south of the volcanic center Lopez Extraña in Tarata's province, Tacna region at an altitude of 4,300 meters. The topography is flat with hills surrounded by mountains. The surface is of soft land with volcanic rocks exposed locally. Geothermal manifestations are characterized by the presence of hot springs, mineral deposits and hydrothermal alterations in the lower valley with a 6km long N-S trend.

In Ancocollo, sedimentary rocks of the basement corresponding to the Huallhuani Formation of Lower Cretaceous outcrop. Above the substrate volcanic rocks, the Tarata Formation of the Paleogene and the Huilacollo Formation and Cumaile - Yenacachi of the Neogene outcrop. Also Inciensocucho volcano of the Quaternary and fluvial deposits and moraines of the Quaternary are present in the area.

Huilacollo Formation has diorite intrusions (De la Cruz et al., 2000). The field is characterized by the presence of several volcanic systems. Although faults are not clearly delineated in the geothermal area and its surroundings in the geological map at 1:50 000 scale (De la Cruz et al., 2000), some faults were identified in the geological field study (Fig.4c). The first (trend NE-SW) is 0.5-0.8 m width with hot springs aligned on these faults; extensive hydrothermal alterations are also observed. (De la Cruz et al., 2000).

The narrow spatial relationship of thermal manifestations and faults, suggests that the permeable zones are developed along faults trending NE-SW and NW-SE and NS observed in the slope of the valley (Fig. 4c). Besides, the thermal manifestations of N-S tendency in the valley indicate the existence of permeable fractures related with the ascent of thermal fluids to the surface. Abundance of Quaternary volcanoes indicates that the heat source is linked to Quaternary volcanic activity.

3.4 Borateras

Borateras is located inside the Maure basin close to the Maure River, in the Tarata province, at an altitude of 4300 m a.s.l. in Tacna Region (Fig. 4e). Climate is cold, dry, with strong sunshine during the day, and low temperatures at nights. There is sparse vegetation, and arid and stony soils can be these observed around the entire zone. The most representative species are Polypelis and Azorella compacta, commonly called Queñuales and Yareta, respectively.

In the zone, there are the presence of a considerable number of geothermal manifestations such as hot springs, boiling springs and mud pools. In October 2007, we carried out a study of the geothermal manifestations with geochemical methods for the interpretation of their chemical and isotopic characteristics.

Borateras is surrounded by a chain of volcanic centers ligned NW-SE. The following recognized volcanic centers are Jaruma, Coverane and Purupuruni, of wich the last one is a group of dacitic domes with a diameter of approximately 850m. These volcanic structures were deposited over the

sedimentary cretaceous, basement composed mainly by interleaving sandstones, limestones and shales. To the south of the field, the mean lithology consists of andesitic lava (with crystals of plagioclase, olivine and pyroxene) interlayered by some porphyritic lavas and sequences of pyroclastic flows. These volcanic deposits range from Upper Miocene to Pliocene and cover almost 90% of the entire zone (De la Cruz et al., 2000).

Some Holocenic deposits are present in this area as alluvials and colluvials, mainly near the river. Some moraines cover the slopes of the Purupuruni domes. Local faults aligned NW-SE constitute the main structure controlling the flow of geothermal waters.

3.5 Kallapuma-Chungara

Kallapuma-Chungara area is located in the oriental part of the Western Cordillera of Andes, E-SE of Borateras geothermal zone in the Tarata province's, at an altitude between 4200 - 4400 m. Around Kallapuma-Chungara area there are volcanic centers, us the Chila volcano located northern part. Climate is cold and dry, the zone is sparsely vegetated.

Various volcanic centers surround Kallapuma-Chungara as Chilla (Fig. 4d), Jucure and Chunape. The dominant lithology of the area consists of andesitic lavas and porphyritic andesites belonging to the Jucure volcanic center of 5.5 My (Diaz et al., 2000). In some sectors the Capillune Formation outcrops, it is composed of yellow-orange layers of reworked sandstones, gray sandstone horizons, limonite and layers of conglomerates cemented by sinter.

In the area close to the Kallapuma riverbed, various Holocene deposits are present, such as fluvial, which are very restricted to the riverbed. These deposits are composed of gravel in a sandy matrix, with some conglomerates cemented by sinter from the hot springs forming large and very compact blocks (Fig. 4d). Fluvioglacial and moraine deposits are widespread in the area; these are composed mostly of poorly selected volcanic fragments without stratification, ranging in sizes from coarse sand to gravel and possibly erratic blocks. The volcanic rocks pertain to the Barroso Group and Pucarani, Barroso of the Neogene (Diaz et. al., 2000).

Presence of faults and fractures trending NS to NE-SW is observed in the geological structure of Kallapuma-Chungara. Some topographic lineaments NE-SW reach the slopes of the mountains (Fig. 4d). There are also young volcanoes inside and around this geothermal area, eg Casiri Snowy, Paucarani Snowy and Cerro Kere (Diaz et al., 2000).

The geological structures and distribution of thermal manifestations indicate that the upward flow of thermal water to the surface would be through the faults. Presence of volcanoes of the medium- late Quaternary around this area, suggests that the heat source would be related to Quaternary volcanic activity.

4. Sampling and analytical techniques

Springs sampling was carried out in five geothermal areas of Tacna region during the period 2009-2010. A total of 31 sets of water samples were collected in plastic bottles of high density. We took 3 samples: One for the analysis of dissolved cations (Li, Na, K, Ca, Mg, B, As, Si) after filtration through a 0.45 µm MILLIPORE filter, was acidified using ultra-pure HNO_3; a second one was taken without addition of acid, to determine anions (Cl, F, SO_4)(non –preserved sample). A third sample, to determine isotopic composition. These samples have enabled us to establish a basis to explain the chemistry of thermal water.

Outlet temperatures (±0.1 °C), pH (±0.1 units) and electrical conductivity were determined in the field using a multiparameter equipment (WTW 340I). Water samples were analyzed in certified and accredited laboratories of Perú and Japan. Isotopic determinations (δ^2H y $\delta^{18}O$) were performed with a Mass Spectrometry (IRMS -MAT 252) and Laser Spectroscopy (Cavity Ring Spectroscopy) LWIA - LGR in the Comisión Chilena de Energía Nuclear (CCHEN) laboratory.

The analyses were as follows: (1) dissolved metals and minor elements (Li, Na, K, Ca, Mg, B, As, Si) by inductively coupled plasma mass spectrometry Agilent 7500. (2) F, Cl, SO_4, by ion chromatography; using a Dionex ICS-2000 Ion Chromatograph and (3) SiO_2 by colorimetry (molybdosilicate method) (4) HCO_3 was analyzed volumetrically by titration with 0.1 N HCl.

Accuracy and precision of the determinations were computed by analyzing certified reference materials and by performing several replicas and samples dilutions. Analytical errors were less than 5%.

5. Results and discussion

Table 1 reports temperature, pH, isotopical and chemical composition of the hot and cold-water discharges from Tutupaca, Calientes, Ancocollo, Borateras and Kallapuma-Chungara geothermal zones. Water temperature range from 7.4°C (CA-9) to 87.3 °C (CA-1), and pH from 2.69 (TU-5) to 8.34 (CA-8). The water of the four hydrothermal systems has similar composition; however, the Tutupaca water chemistry is different being acidic most of the hot springs. The dominant anions in most water samples is either Na^+ and Cl^-, whereas those of Tutupaca have relatively high SO_4^{2-}, Ca^{2+} and Mg^{2+} concentrations in comparison to the other four zones.

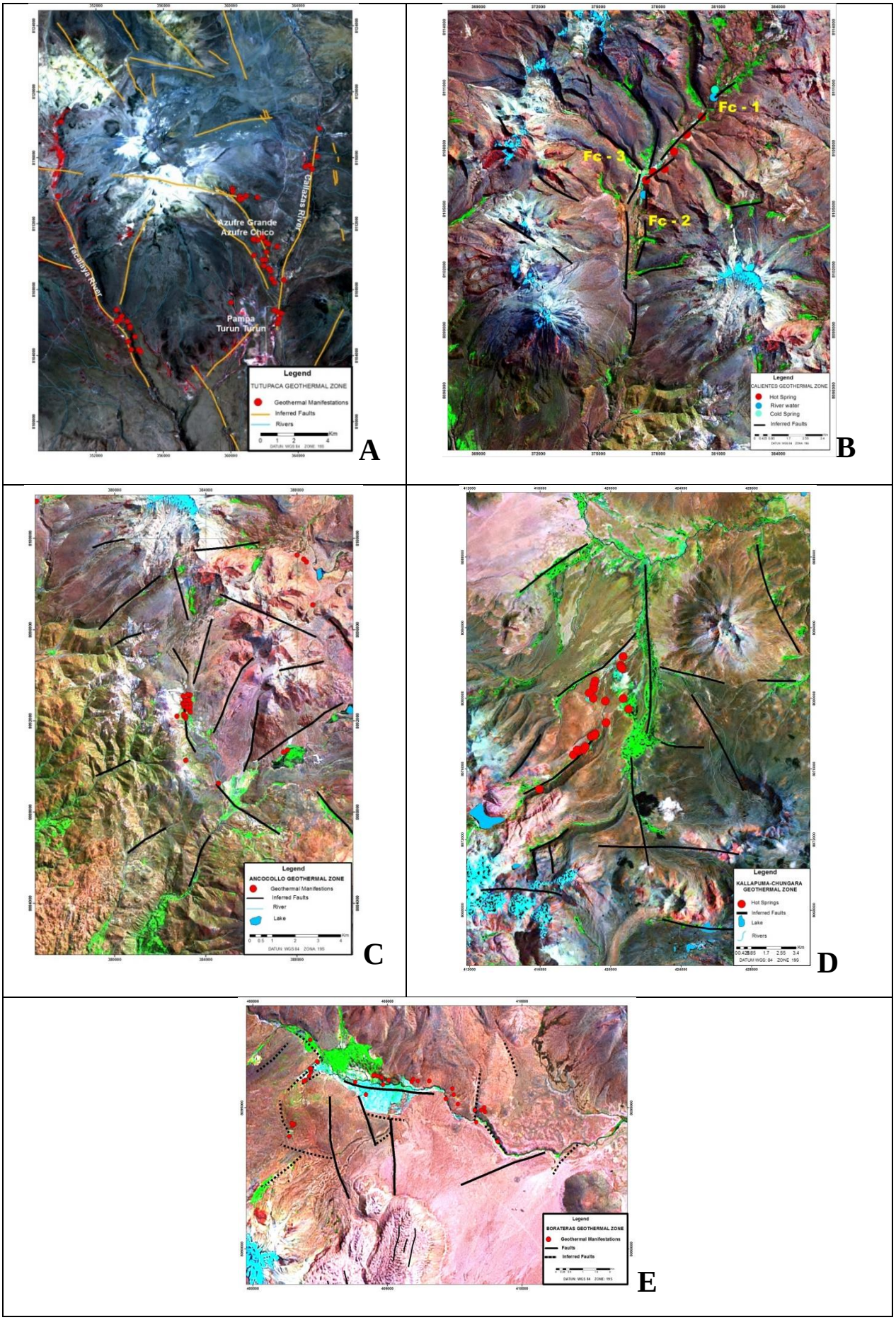

Fig. 4. Schematic location map of the geothermal areas: a) Tutupaca, b) Calientes, c) Ancocollo, d) Kallapuma-Chungara and e) Borateras; and location of the sampling sites.

Table 1: Outlet temperatures (in °C), pH, concentrations of main ions and minor species and $\delta^{18}O$ and $\delta^{2}H$ (‰V-SMOW) values of the thermal discharges from the Tutupaca (TU),Calientes (CA), Ancocollo (AN), Borateras (BO) and Kallapuma-Chungara (KC) hydrothermal systems, Tacna region, southern Perú. Concentrations of solutes are in mg/L, n.a.: not analyzed; n.p: not present.

Sample	Code	Cord N	Cord E	Altitude	T (°C)	pH	Li	Na	K	Ca	Mg	B	As	SiO2	Cl	SO4	HCO3	F	$\delta^{2}H$ (‰)	$\delta^{18}O$ (‰)	$\delta^{34}S(SO_4)$ (‰)	$\delta^{18}O(SO_4)$ (‰)
Azufre Grande-1	TU-1	8110991	361601	4339	62.6	2.9	1	310	24	185	42	6	2	213	179	1206	n.p.	5	n.a.	n.a.	n.a.	n.a.
Tacalaya -1	TU-2	8104850	353918	4070	57.8	6.9	2	639	47	65	8	12	1	125	415	412	662	1	n.a.	n.a.	n.a.	n.a.
Azufre Grande	TU-3	8110994	361608	4335	61.9	2.71	n.a.	173	25	156	42	6	n.a.	214	190	1082	n.a.	n.a.	-105	-15	n.a.	n.a.
Tacalaya	TU-4	8104852	353916	4064	57.7	6.91	2	590	42	55	6	12	n.a.	120	421	379	575	n.a.	-103	-14	n.a.	n.a.
Azufre Chico	TU-5	8110078	361376	4307	49.3	2.69	1	196	16	127	34	4	2	n.a.	160	1214	n.p.	n.a.	n.a.	n.a.	n.a.	n.a.
Azufre Grande	TU-6	8111019	361376	4330	61.6	2.76	1	173	22	138	37	5	2	n.a.	182	1151	n.p.	n.a.	n.a.	n.a.	n.a.	n.a.
Azufre Chico	TU-7	8111070	361347	4390	49.8	n.a.	0.7	190	17	153.0	43.00	n.a.	n.a.	222	257	1090	n.p.	n.a.	n.a.	n.a.	n.a.	n.a.
Azufre Grande	TU-8	8111166	361879	4310	66.1	4.5	0.7	185	23	150.0	40.00	n.a.	n.a.	216	271	1033	n.p.	n.a.	n.a.	n.a.	n.a.	n.a.
Azufre Grande	TU-9	8110276	362121	4270	63.3	4.5	2.8	450	75	89.0	21.00	31	n.a.	298	735	592	n.p.	n.a.	n.a.	n.a.	n.a.	n.a.
Azufre Grande	TU-10	8108435	362607	4220	47.6	4.5	1	250	50	138.0	33.00	n.a.	n.a.	121	354	816	n.p.	n.a.	n.a.	n.a.	n.a.	n.a.
Rio Callazas	TU-11	8108592	363167	4100	52.1	6.5	1.3	248	30	52.0	23.00	62	n.a.	165	353	195	672	n.a.	n.a.	n.a.	n.a.	n.a.
Tacalaya Sur	TU-12	8106065	353224	4140	46	6.5	1.9	450	34	50.0	6.00	14	n.a.	107	490	319	903	n.a.	n.a.	n.a.	n.a.	n.a.
Tacalaya Sur	TU-13	8104231	354655	4090	55.3	6.5	2.5	600	40	66.0	6.00	n.a.	n.a.	130	622	409	793	n.a.	n.a.	n.a.	n.a.	n.a.
Turun Turun	TU-14	8107219	360014	4225	25.5	5.5	0.2	83	14	63.0	24.00	7	n.a.	130	61	201	749	n.a.	n.a.	n.a.	n.a.	n.a.
Calientes	CA-1	8109551	380218	4423	87.3	7.60	11	1190	112	52.5	0.235	54.8	8.66	263	1900	60.2	117	3.62	-117	-13.6	6.5	-7.4
Calientes	CA-2	8108726	379431	4389	81.7	7.44	n.a.	1180	88.3	32.5	0.242	53.4	6.33	258	1860	84.1	83	n.a	n.a.	n.a.	n.a.	n.a.
Calientes	CA-3	8107828	378788	4362	86.6	6.90	n.a.	774	55.4	45.6	3.87	32.1	5.01	204	1110	99.1	195	n.a	n.a.	n.a.	n.a.	n.a.
Calientes	CA-4	8106970	378315	4359	54.8	7.53	n.a.	n.a.	n.a.	n.a.	n.a.	n.a.	n.a.	141	271	21	123	n.a	n.a.	n.a.	n.a.	n.a.
Calientes	CA-5	8106907	377296	4328	84.3	7.12	9.75	1180	51.6	39.1	0.224	52.7	7.88	248	1810	128	53	3.34	-115	-13.3	10	-6.3
Calientes	CA-6	8106407	377398	4312	84.3	7.90	n.a.	1120	48.6	33.5	0.043	49.8	8.33	297	1700	122	78	n.a.			n.a.	n.a.
Calientes	CA-7	8110846	380888	4491	26.9	7.24	n.a.	n.a.	n.a.	n.a.	n.a.	n.a.	0.084	n.a.	3.05	n.a.	n.a.	n.a.	-122	-16.1	n.a.	n.a.
Rio Calientes	CA-8	8105687	377268	4293	23.8	8.34	n.a.	n.a.	n.a.	n.a.	n.a.	n.a.	3.93	n.a.	1170	n.a.	n.a.	n.a.			n.a.	n.a.
Rio Calientes	CA-9	8110754	380992	4476	7.4	3.40	n.a.	n.a.	n.a.	n.a.	n.a.	0.26	<0.005	n.a.	8.17	479	n.a.	n.a.	-111	-15.4	n.a.	n.a.
Ancocollo I	AN-1	8092213	383047	4177	84	6.53	9	1196	115	46	2	46	6	157	1951	215	84	3	n.a.	n.a.	n.a.	n.a.
Ancocollo II	AN-2	8092213	383047	4177	85	7.35	9	1317	110	43	1	49	8	188	1895	234	185	2	n.a.	n.a.	n.a.	n.a.
Ancocollo-1	AN-3	8092635	383047	4200	85.8	8	10	1310	117	38	1	50	n.a.	182	1951	210	92	n.a.	-115	-14	n.a.	n.a.
Collpapampa	AN-4	8089267	384569	3992	71.2	7.02	n.a.	535	98	139	30	21	n.a.	253	763	585	59	n.a.	-108	-14	n.a.	n.a.
Putina Chico A	BO-1	8096345	402170	4376	86	7.9	12.2	1310	91	68	0.484	95.4	14.8	255	2150	71.9	86	1.99	-106	-11.1	9	-5.7
Putina Chico B	BO-2	8096132	402102	4363	82.5	7.5	n.a.	1020	96.3	44.4	2.84	72.7	9.42	233	1630	70.3	93	n.a	-109	-12.3	n.a.	n.a.
Calachaca	BO-3	8094494	408299	4295	43.6	7.3	n.a.	253	29.5	36.8	17	16.5	1.85	133	350	37.1	224	n.a	-119	-15.8	4.5	-1
Pozo pampa Boratera	BO-4	8095464	404204	4326	59	7.3	4.29	643	77.2	40.1	9.17	43.4	5.64	176	981	73.3	128	0.51	-114	-13.9	n.a.	n.a.
Fuente a lado del Rio Maure	BO-5	8095316	407177	4304	47.3	7.2	n.a	592	68.1	45.2	13	39.6	4.83	169	874	66.3	184	n.a.	-126	-17.1	n.a.	n.a.
Putina Grande	BO-6	8093998	401357	4535	72.2	6.9	n.a.	n.a.	n.a.	n.a.	n.a.	n.a.	n.a.	127	0.38	47.6	21	n.a	n.a.	n.a.	n.a.	n.a.
Villachaullani	BO-7	8097405	402135	4362	12.4	7.7	n.a.	n.a.	n.a.	n.a.	n.a.	n.a.	0.02	n.a.	0.88	n.a.	n.a.	n.a.	n.a.	n.a.	n.a.	n.a.
Rio Maure	BO-8	8093808	409097	4281	25.2	7.6	n.a.	n.a.	n.a.	n.a.	n.a.	n.a.	2.28	n.a.	510	n.a.	n.a.	n.a.	n.a.	n.a.	n.a.	n.a.
Junto Pujo	KC-1	8080411	420279	4332	69	6.25	5	841	110	45	16	40	12	170	1277	117	192	1	n.a.	n.a.	n.a.	n.a.
Chungará	KC-2	8077133	418719	4441	82.2	6.67	7	1142	113	50	4	58	18	109	1823	165	166	2	n.a.	n.a.	n.a.	n.a.
Chungará-1	KC-3	8076872	418346	4456	84.6	7	8	1263	117	59	5	67	n.a.	110	1978	147	171	n.a	-111	-14	n.a.	n.a.
Juntopujo-1	KC-4	8080410	420280	4341	70.7	7	5	835	93	43	12	39	n.a.	165	1279	105	180	n.a	-116	-15	n.a.	n.a.

The thermal springs directly associated with the hydrothermal system, have concentrations of Na^+ and K^+ ranging from 83 to 1317mg/L and 14 to 117mg/L respectively. Also these springs reach high concentrations of Cl^- up to 2150 mg/L and B up to 95.4 mg/L. Very low concentrations were measured of some chemical species like NO_3^-, I^- and NO_2^- (not included in the tables). Electrical conductivities (CE) range from 0.01 to 7.94 mS/cm.

Most of these springs show bubbles indicating the presence of dissolved CO_2, which forms HCO_3^- upon reaction with the host rocks resulting in concentrations between 8 mg/L and 903mg/L. Sulfate concentrations range from 21mg/L to 1206mg/L. Chloride$^-$ is the dominant ion followed by sodium. Waters are mainly neutral Na^+ - Cl^- type, typical of the deep geothermal fluids found in most high-temperature systems. Relatively high concentrations of Li^+ and As^+ up to 12.2mg/L and 18 mg/L respectively are also present in these springs. Concentrations of SiO_2 vary between 109 and 298 mg/L.

5.1 Water Chemisrty

Samples were classified by using hydrochemical diagrams. According to the Langelier Ludwig diagram (Fig. 5) the water chemistry shows the existence of three water types; most of the thermal samples are located in the Na-Cl sector. This indicates that waters are sodium-chloride or alkaline type, characteristic of geothermal waters. In addition, the

diagram shows that the Tutupaca samples correspond to Ca-SO_4 type and have an acidic pH; some of them corresponding to a Ca-HCO_3 type indicate mixing with superficial waters.

The Giggenbach diagram (Fig. 6)(Giggenbach, 1991), shows that the geothermal waters from the four areas (Calientes, Ancocollo, Borateras and Kallapuma-Chungara) plot close to the chlorine corner in the field of mature geothermal waters. These result likely from the discharge of the neutral chloride geothermal reservoir and represent equilibrated fluid. Tutupaca springs as shown by the ternary diagram are volcanic and peripheral geothermal waters. In this area possibly, steam heated waters were formed as a result of absorption of magmatic gases into ground water and are characterized by a low pH (Giggenbach, 1988). The peripheral bicarbonate waters with high carbon dioxide content are of near-neutral pH, which reacted with the local rocks either in the shallow reservoir or during lateral flow (Nicholson, 1993).

A Piper trilinear diagram (Fig. 7) also shows that most of the hot springs are Na-Cl type. These hot springs are associated to geothermal zones of Calientes, Ancocollo, Borateras y Kallapuma-Chungara. The anions dominant for geochemical facies for these samples are Na and Cl; probably resulted from water-rock interaction processes. While in Tutupaca the hydrochemical composition of some hot springs is Ca-SO_4 and high in Mg possibly associated with acid volcanic fluids of the Tutupaca volcanic complex located close to the geothermal area. Around most of Tutupaca acidic hot springs, yellow, red and whitish colored sulfur precipitates are present. These precipitates may have been produced from: (1) precipitation of SO_4^- minerals (mainly gypsum, alunite and jarosite) and elemental S; and (2) bacterial reduction of SO_4^{2-} to S^{2-} and precipitation of sulfide minerals. However, the rock leaching process in the zone may be negligible as indicated by their low Li concentrations (Martini et al., 1994).

Chemical types and mineralization of geothermal waters reflect the geochemical processes of water–rock interaction and the chemistry of the rocks through which waters circulate. Most of the geothermal waters in Tacna region are Na-Cl and Ca-SO_4 types; some are other types like Ca-Mg-SO_4, Na-Cl-SO_4, Ca-HCO_3, Na-HCO_3 and Na-K-Cl (Cruz et al., 2013).

Figure 8 shows that the waters of geothermal zones in Tacna region interacted with marine sedimentary rocks at deep levels, which probably have relatively high porosity and permeability with abundant fractures (Shigeno et al., 1993; Shigeno and Abe 1983). It is possible that hot waters in the five zones (Tutupaca, Calientes, Ancocollo, Borateras and Kallapuma-Chungara) interacted and leached boron-bearing host rocks due to relatively deep circulation paths. Excessively high boron concentrations have been documented for geothermal systems flowing through boron-rich sedimentary rocks (e. g, Aggarwal et al., 2003).

On the other hand, the high B concentration may be possibly related with young volcanism, in this case with actives volcanoes like part of the Quaternary volcanic arc, associated with dissolution of volcanic gases in the hot water influenced by magmatic gases where B and Cl form volatile compounds. This could also indicate that in the studied geothermal areas, the higher B/Cl ratio could be favored by magmatic heating or cooling intrusions (Arehart et al., 2003).

The Cl-Li-B ternary diagram (Giggenbach, 1992) can be used to examine the possible origin of Cl and B in geothermal waters as conservative tracers due to minor modifications of their composition by secondary alteration processes. These waters are likely derived from the incorporation of magmatic volatiles (HCl and H_3BO_3), while Li is released during water-rock interactions (rock dissolution) and intimately dependent on temperature (e.g. Fouillac and Michard, 1981; Giggenbach & Goguel, 1989).

Figure 9 shows the Li-Cl-B composition of samples, where some waters have tendency towards the Cl^- corner and others to B. This could indicate that most of the geothermal systems have volcanic-magmatic associations. The water chemistry may be explained in terms of rock dissolution in deeply flowing groundwater enriched with high temperature, high pressure magmatic vapors. These vapors may contain Cl^- and B in proportions close to those of the contacted crustal rocks (Giggenbach, 1989). One sample of the Tutupaca area close to the B corner may have originated from a relatively young hydrothermal system with absorption of high B/Cl magmatic vapors. Furthermore, the concentration of B in the geothermal waters ranges from 0.26 to 95.4 mg/L, with atomic ratio B/Cl of 0.08 to 0.58 indicating that waters interacted with different lithologies at depth associated to sedimentary rocks (Fig.8).

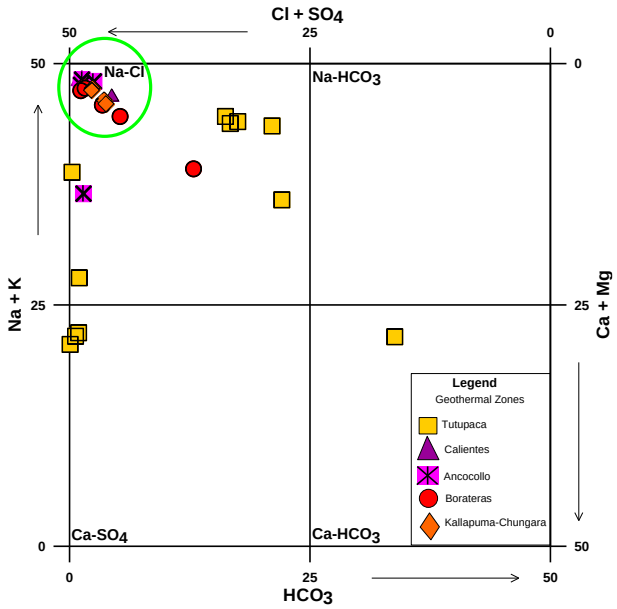

Fig. 5. Langelier-Ludwig diagram for thermal springs.

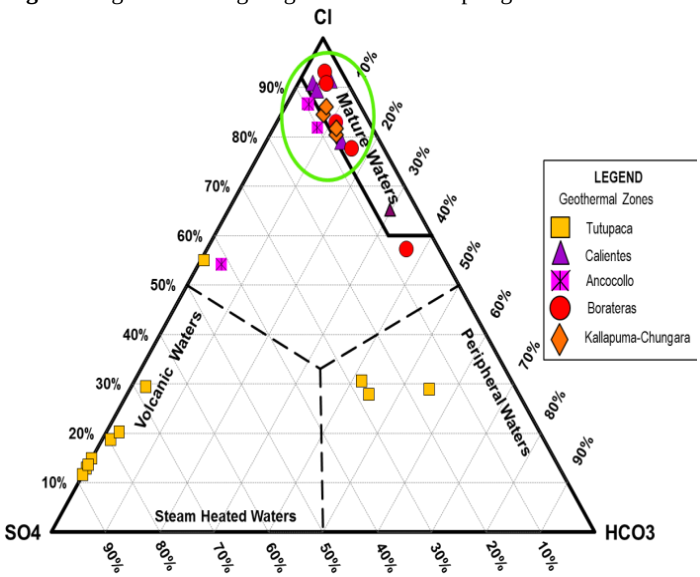

Fig. 6. Cl-SO_4-HCO_3 ternary diagram (Giggenbach and Goguel, 1989).

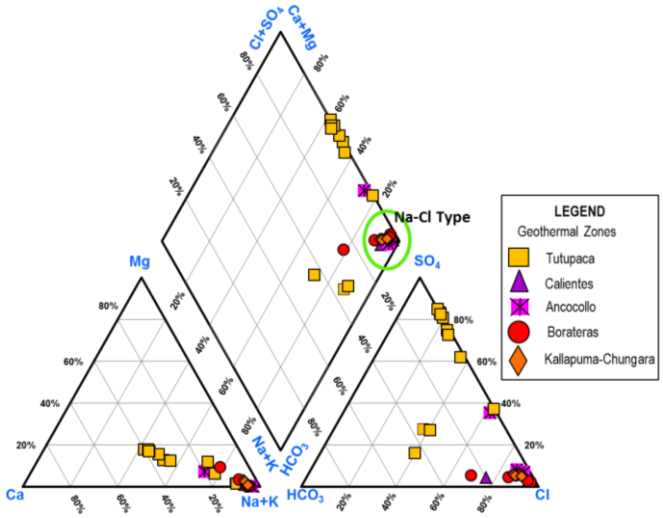

Fig. 7. Piper-Hill diagram for the chemical composition of the thermal spring.

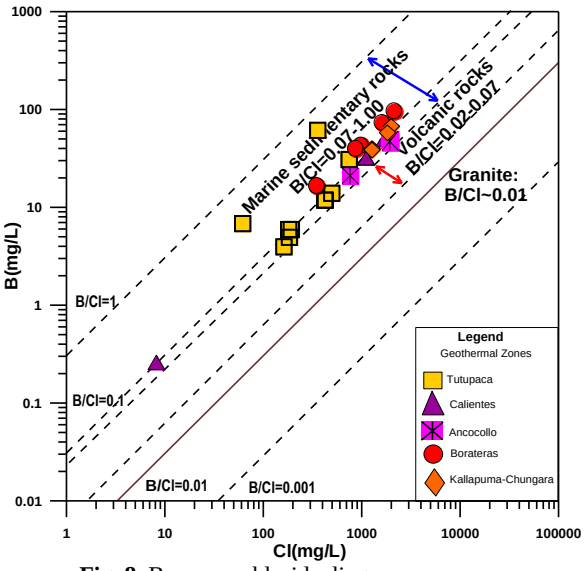

Fig. 8. Boron vs chloride diagram.

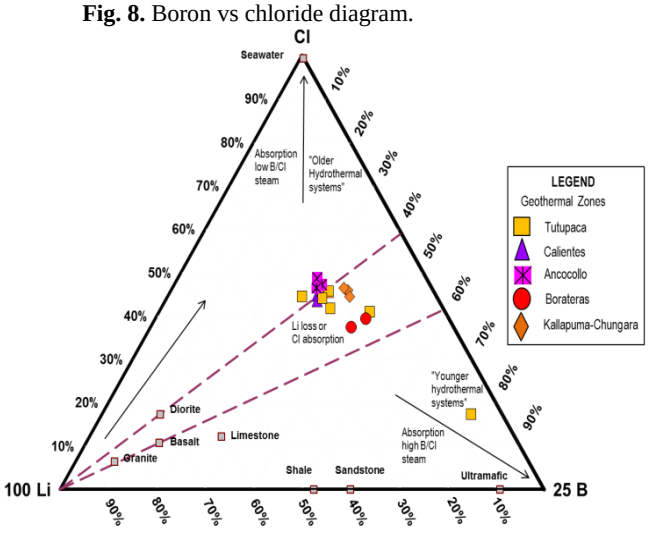

Fig. 9. Cl-Li-B ternary plot of thermal waters (Giggenbach, 1991a).

5.2 Chemical geothermometry

Na-K-Mg diagram

The Na–K–Mg diagram of Giggenbach (1988) (Fig. 10) uses a combination of Na–K and K–Mg geothermometers to obtain Na-K and K-Mg equilibrium temperatures of fully equilibrated waters (Joseph et al., 2013). The different temperatures resulting from the application of the geothermometers (Table 2) are related to the rate of re-equilibration during fluid–rock interactions where Na has the slowest rate, K an intermediate, and Mg a rather fast one. Hence Na–K shows always deep equilibrium (usually with the highest temperature), and K–Mg relates to shallower equilibration (usually with lower temperature). This method only describes equilibration processes at different levels and up-flow rates in a thermal reservoir. As shown in Table 2, the results vary within a wide range.

From Fig. 10, it can be seen that most thermal waters of deep circulation (e.g., Calientes, Ancocollo, Boraters, Kallapuma-Chungará) plot on the full and partially equilibrium lines which means that these waters have attained equilibrium between water and rock. While Tutupaca waters are located in the immature waters field close to the Mg corner indicating

water–rock interactions during their flow, or mixing with cold groundwater that has not yet reached ionic equilibrium.

However, the higher concentrations of Mg also indicates near-surface reactions leaching Mg from the local rock, or dilution by groundwater, which can be relatively Mg- rich (Nicholson, 1993). In the case of Azufre Grande, Azufre Chico and Turun Turun the hot springs are acidic. The high percentage of Mg could thus be related to rock leaching favored by a low-pH.

The Na-K-Mg diagram indicates a linear trend pointing to a Na/K equilibrium temperature over 200°C in the reservoir. The linear trend is either due to dilution or to mixing.

K-Mg-Ca geoindicator diagram

The "geo-indicator" or the K–Mg–Ca geothermometer proposed by Giggenbach and Goguel (1989) is plot in Figure 11. According to Giggenbach, It is likely that the initial CO2 contents of deep geothermal fluids are externally controlled by variable contributions of CO_2-rich magmatic fluids and C02 from meteoric water. These fluids are expected to become reactive in the formation of calcite from Ca-Al-silicates, which involves the formation of "acid clays". The reaction governing CO_2 pressure in a "full equilibrium" system corresponds to the following Eq. (1):

Equation (1)
Ca–Al_2–silicate + K-feldspar + CO_2 ↔ K-mica + calcite

In the diagram (Fig. 11), the Calientes and Borateras waters with slightly alkaline pH, plot above the full equilibrium line, expressing the coexistence of K-feldspar, illite and chlorite, with CO_2 contents too low to induce rock alterations as expressed in Eq. (1), implying that the CO_2 contributing to magmatic fluids has been affected by dilution with meteoric waters. The samples fall below the full equilibrium line but plot on the line separating calcite formation and immature water fields, indicating, that have PCO_2 higher than full-equilibrium PCO_2, and can promote conversion of Ca-Al-silicates to calcite. Also other samples plot below the lower boundary for calcite formation indicating that the fluids may have risen too fast for calcite alteration to take place (Giggenbach, 1988; Joseph et al., 2013). This indicates that the composition of these waters at their last equilibration temperatures (tkm) was exclusively controlled by CO_2 concentrations (Mutlu, 1998).

Na-K-Mg-Ca diagram

Other evaluation of temperature and fluid–rock equilibrium based on the ionic geothermometer in the Na-K-Mg-Ca system (Giggenbach, 1988) is represented in the 10Mg/(10Mg+Ca) vs 10K/(10K+Na) diagram (Fig. 12). In this diagram the curves of the water composition expected for equilibrium with an average crustal rock (Giggenbach, 1984), and that produced via isochemical dissolution of crustal rocks are plotted (Tassi et al., 2010).

Plotting of Tacna samples in the diagram (Fig. 12) indicates partially and fully equilibration between water and rock. For example again some samples of the Calientes and Borateras zones have reached full equilibrium at about ~175-230°C (blue circle). However, other water samples from the Tacna region are closer to the complete equilibrium line from fluid-rock interaction, such as Ancocollo and Kallapuma-Chungara waters, which is consistent with their plotting in Figure 10. Besides, if making a vertical projection of the equilibrium line, the liquid would be exposed to different temperatures from ~175 to above 240 °C.

SiO2 vs. log(K_2/Mg) diagram

Silica concentrations in geothermal fluids are controlled by the solubility of the different silica minerals. The sampled waters of the geothermal zones in Tacna region have values from 109 to 298 mg/L. To assess the solubility variation of the solid SiO_2 species involved in the equilibration of geothermal waters the K, Mg and SiO_2 data were plotted in the SiO_2 vs Log(K^2/Mg) diagram together with the solubility curves for amorphous silica, beta cristobalite , chalcedony, and quartz (Fig. 13). The figure shows that the sampled waters plot along the alpha cristobalite, chalcedony and quartz curves. Some samples from Calientes, Ancocollo and Kallapuma-Chungara lie on the quartz curve.

Temperatures obtained from the solubility of SiO_2 vary from 84 to 206°C. The Calientes, Borateras and Kallaguma-Chungara zones waters have the highest reservoir temperature ranging from 146 to 206 °C (Fig. 13) the rest of the samples possibly resided in a high temperature reservoir. This suggests that the disagreement between the silica and cation geothermometers can only partially be related to SiO_2 precipitation at decreasing temperature along the fluid ascending pathways or that the hydrothermal fluids are diluted by relatively cold shallow aquifers.

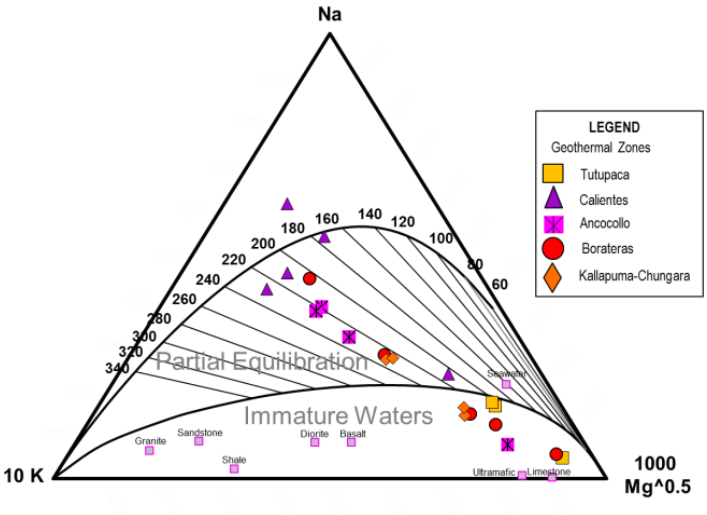

Fig.10. Graphical evaluation of water-rock equilibrium temperatures for thermal waters using Na-K-Mg concentrations.

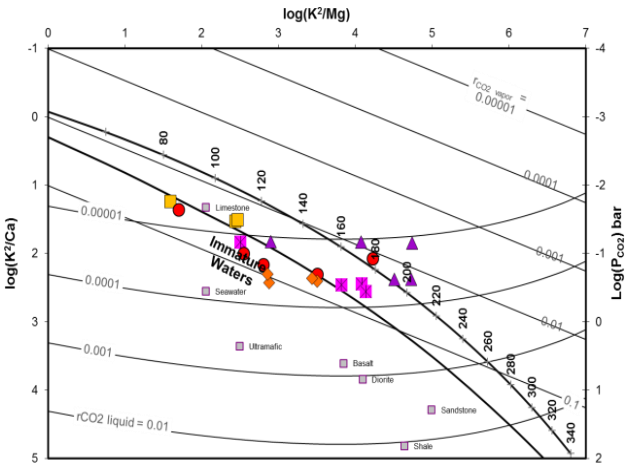

Fig. 11. Plot of log (K2/Mg) vs. log (K2/Ca), used to evaluate the PCO_2 of geothermal liquids (Giggenbach, 1988).

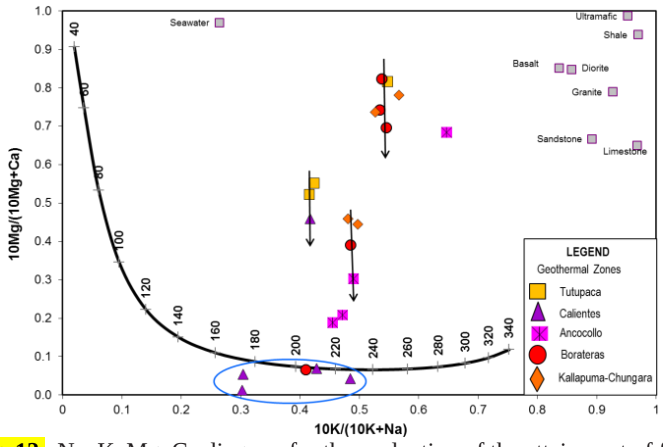

Fig. 12. Na–K–Mg–Ca diagram for the evaluation of the attainment of full equilibrium (blue circle) with average crustal rock (Giggenbach, 1988).

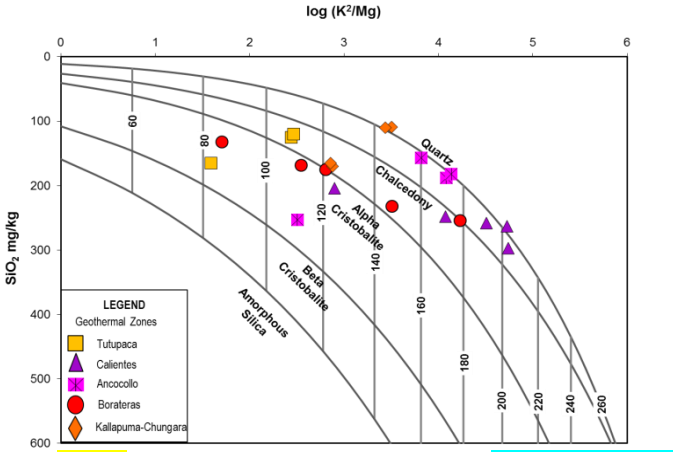

Fig.13. Plot of SiO_2 vs. log(K^2/Mg) (from Giggenbach et al., 1994, modified).

Table 2. Estimated temperature (in °C) for thermal waters discharge from the Tutupaca (TU),Calientes (CA), Ancocollo (AN), Borateras (BO) and Kallapuma-Chungara (KC) hydrothermal systems, Tacna region, southern Perú using geothermometers.

Hot spring	Code	Amorpho us Silica	Alpha Cristoba lite	Beta Cristoba lite	Chalcedony conductive	Quartz conductive	Quartz adiabatic	Na-K-Ca	Na-K-Ca Mg corr	Na/K Fournier 1979	Na/K Truesdel l 1976	Na/K Giggenbach 1988	Na/K Tonani 1980	Na/K Nieva & Nieva 1987	Na/K Arnorsson 1983	K/Mg Giggenbach 1986
Azufre Grande-1	TU-1	60	135	85	164	185	172	91	73	196	162	213	194	183	170	71
Tacalaya -1	TU-2	29	100	51	125	150	143	177	120	192	157	209	188	179	166	110
Azufre Grande	TU-3	61	135	85	164	185	172	90	66	251	231	264	272	237	236	72
Tacalaya	TU-4	26	97	48	122	148	141	176	127	189	154	207	185	177	163	111
Azufre Chico	TU-5							81	69	200	167	217	200	187	175	64
Azufre Grande	TU-6							88	67	238	215	252	254	225	221	70
Azufre Chico	TU-7	63	138	88	167	188	174	79	68	208	176	224	210	195	184	63
Azufre Grande	TU-8	61	136	86	165	186	172	89	67	236	212	250	251	223	218	71
Azufre Grande	TU-9	84	161	110	193	210	191	215	91	265	250	277	294	251	254	110
Azufre Grande	TU-10	27	98	49	123	148	142	209	76	285	277	294	324	270	278	92
Rio Callazas	TU-11	44	117	68	144	168	158	189	41	234	209	248	247	220	215	84
Calientes	CA-1	75	151	101	181	200	184	205	205	212	181	228	216	199	189	205
Calientes	CA-2	74	149	99	180	199	183	196	196	193	158	210	190	181	167	194
Calientes	CA-3	58	132	82	160	182	169	182	149	190	154	207	185	177	163	126
Calientes	CA-4	35	107	58	133	158	150									
Calientes	CA-5	71	146	96	176	196	180	165	165	155	113	174	140	143	123	173
Calientes	CA-6	84	160	110	192	210	191	165	165	155	112	173	139	143	123	206
Ancocollo I	AN-1	41	114	64	141	164	155	208	199	214	183	229	218	201	191	162
Ancocollo II	AN-2	52	126	76	154	176	165	202	202	202	169	218	202	189	177	174
Ancocollo-1	AN-3	50	124	74	152	174	163	207	207	207	176	223	210	194	184	176
Collpapampa	AN-4	72	148	98	178	198	182	167	83	275	263	286	309	261	266	112
Putina Chico A	BO-1	73	148	98	179	198	182	187	187	188	151	205	182	175	161	181
Putina Chico B	BO-2	66	141	91	171	191	177	204	183	212	181	228	216	199	189	149
Calachaca	BO-3	32	103	54	129	154	147	140	43	231	205	245	242	217	211	87
Pozo pampa Boratera	BO-4	48	121	72	149	172	161	210	115	233	208	247	246	220	214	123
Fuente a lado del Rio Maure	BO-5	46	119	69	146	169	159	189	86	229	203	244	240	216	210	114
Junto Pujo	KC-1	46	119	69	146	170	159	220	96	241	218	255	258	227	224	125
Chungará	KC-2	21	91	43	116	142	137	208	179	216	186	231	222	203	194	149
Chungará-1	KC-3	22	92	43	116	143	137	204	171	211	179	226	214	197	187	146
Juntopujo-1	KC-4	44	117	68	144	168	158	210	105	226	199	241	236	213	206	124

5.3 Mixing Model

These models aim to obtain a preliminary idea of the geothermal potential based on the geological and geochemical results; however the actual potential should be evaluated based on drilling boreholes. The silica-enthalpy and chloride-enthalpy mixing models prosed by Truesdell and Fournier (1977) and Fournier (1979), respectively, were applied in our study to examine the subsurface temperatures of mixed hot spring waters. In these models, enthalpy is used as a coordinate rather than temperature, because the combined heat contents of two waters at different temperatures are conserved when those waters are mixed, but the combined temperatures are not (Burgos, 1999). The corresponding enthalpies are related to the on site temperatures of the geothermal fluids after Fournier and Potter (1982). Enthalpy values were determined using the steam tables of Keenan et al. (1969).

The quartz geothermometer enthalpy-chloride plot (Fig. 14) shows a clear grouping of hot spring along the dilution trend; however the figure shows that the springs have a trend to the boiling line. Also Figure 14 demonstrates that hot spring waters from the four geothermal areas (Calientes, Ancocollo, Borateras and Kallapuma-Chungara) are slightly high enthalpy systems. Assuming the existence of hot fluid with a temperature over 200°C at depth, it is suggested that the spring waters are derived from cooling of this hot fluid through conductive cooling, steam separation by boiling or minor dilution by cold groundwater. However, the water samples from Tutupaca geothermal system have low enthalpy and chloride concentrations suggesting that the hydrothermal fluids result from the mixing of hot water with cold and low Cl^- ground and/or river waters.

In the silica-enthalpy diagram (Fig. 15), the silica concentrations of the samples were plotted against their corresponding enthalpies. Extrapolation of the lines through the data points indicates that temperature goes up to 234°C; however Figure 15 shows that hot springs do not intersect the solubility curve, possibly due to two reasons. One is that the hot springs waters have cooled conductively without losing silica, thus shifting the data points to the left on the diagram making the line describing the silica-enthalpy relationship too steep. The other possibility is that the waters have boiled before mixing (Arnórsson, 2000).

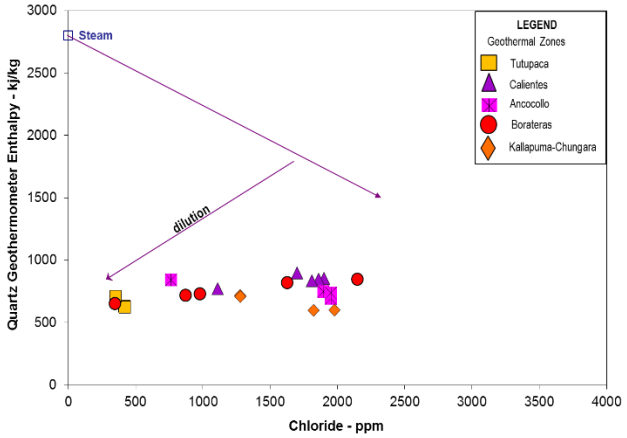

Fig. 14. Quartz Geothermometer enthalpy vs. chloride in thermal waters (Truesdell and Fournier, 1977).

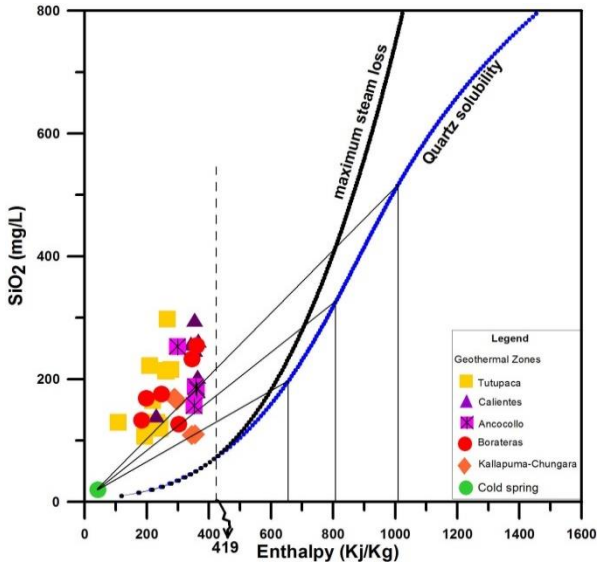

Fig. 15. Mixed model SiO_2-Enthalpy for geothermal water samples.

5.4 Stable isotopes

An early result of the application of stable isotopic techniques to hydrothermal system was Craig's finding about the success of this technique for understanding the complexity of hydrothermal systems (Valley et al., 1986).In a δ^2H versus $\delta^{18}O$ plot (Fig. 16), thermal waters range from -16.1 to -12.3‰ for $\delta^{18}O$, and from -126 a -103‰ for δ^2H. The hot spring samples show negative $\delta^{18}O$ and plot close to the local meteoric line (Cortecci et al., 2005) indicating that these waters are mainly fed by meteoric water. Possibly, the geothermal reservoir waters originate from a mixture of meteoric and magmatic water. However, samples from Tutupaca geothermal zone are located on the meteoric line.

The main geothermal reservoirs in the geothermal zones of the Tacna region do not show isotopic exchange of the feeding meteoric water with rocks, but their isotopic composition may be interpreted as deriving from mixing of meteoric precipitation from the Andean Cordillera with andesitic-magmatic waters (Fig. 16). The isotopic trends of Borateras, Ancocollo, Kallapuma-Chungara and Calientes waters converge towards the isotopic composition of andesitic waters (Taran et al., 1989; Giggenbach, 1992).

Therefore, hydrogen and oxygen isotopic composition and Cl concentration of the spring waters in the four geothermal zones in Tacna region indicates that geothermal reservoir waters originate likely from a mixture of meteoric and magmatic waters (Figs. 17 and 18). However, the mixing ratio of magmatic water (andesitic water) is estimated only around 24 to 25% for Borateras, Ancocollo, Kallapuma-Chungara and Calientes, thus the main constituent is meteoric water infiltrated to the subsurface from the Andean Cordillera. In this mixing model, the Cl concentration of magmatic water contributing to the reservoir is assumed to be about 8,000 mg/kg. The hydrogen isotopic ratio of meteoric water, possibly the main source of the reservoir water, seems to be smaller than the cold spring waters, so that the meteoric water is thought to have infiltrated at a considerably higher elevation than the Maure river area.

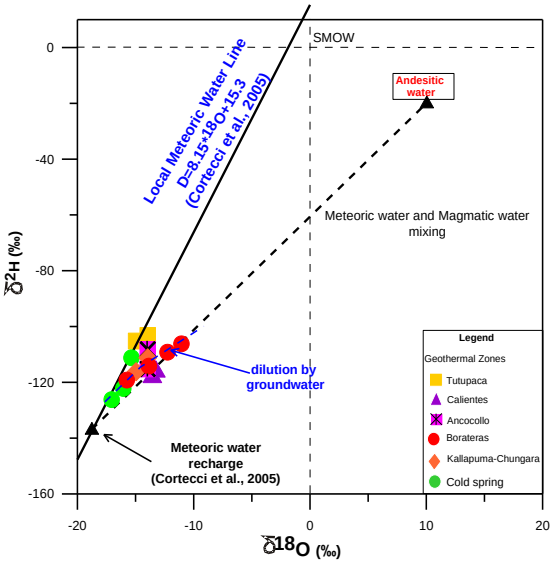

Fig. 16. δ^2H versus $\delta^{18}O$ relation for hot and cold waters from this work. The data are compared with the meteoric water line (MWL, $\delta^2H = 8.15\ \delta^{18}O+15.3$; Cortecci et al., 2005).

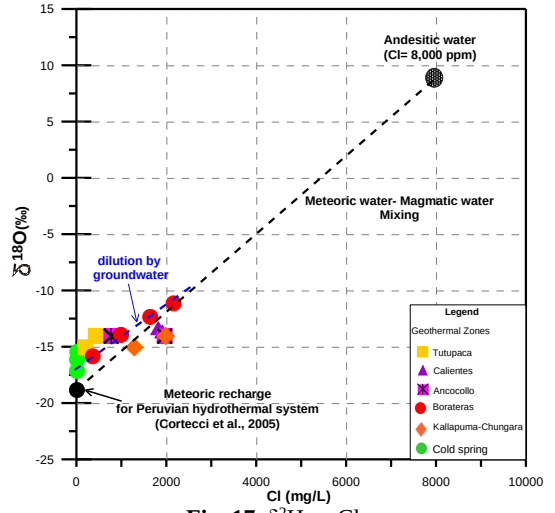

Fig. 17. δ^2H vs Cl.

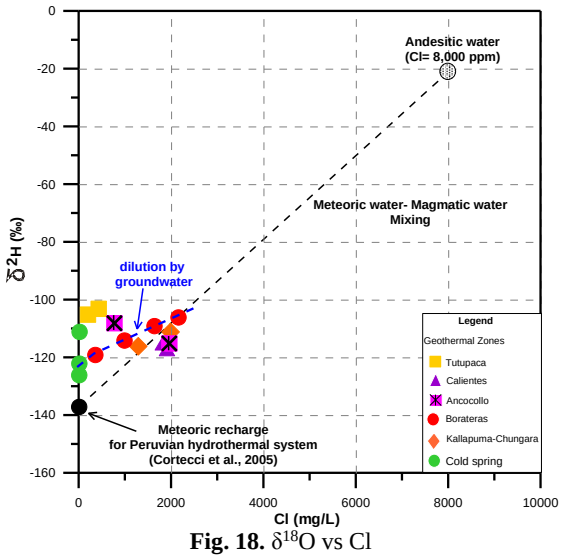

Fig. 18. $\delta^{18}O$ vs Cl

6. Conclusions

In the Tacna region, the geothermal manifestations are associated with active Quaternary volcanism of the Andean cordillera in southern Peru. The geochemistry characterization of the thermal waters discharging in the five studied areas, defines basically Na^+-Cl^- and Ca^{2+}-SO_4^{2-} water types, but the main water type emerging in these areas corresponds to sodium chloride or mature waters. The Cl^- comes from the deep reservoirs, where strong dissolution of the surrounding rocks produces large sodium contributions. This composition results from a 3 end-members mixing: 1) A deep chloride reservoir, 2) A component of meteoric water, and 3) A component of volcanic fluids, also is probably mixed by shallow cold groundwater during ascending process. The compositions of the thermal waters reveal that they have reached rock-water chemical equilibrium. The relatively high boron concentrations in the geothermal waters may be due to deep circulation paths, that interacted with different lithologies at depth associated to Mesozoic marine sedimentary rocks, also associated to andesitic volcanic rocks. Accordingly, the stable isotope relationship between $\delta^{18}O$ and δ^2H suggests that the geothermal waters are a mixture of meteoric and magmatic waters. The reservoirs are liquid dominant.

Application of liquid phase geothermometers to calculate the temperature of the geothermal reservoir for the five areas, indicate that in most cases the reservoir temperatures exceed 200°C.

Acknowledgemenst

This work stems as part of a geothermal studies programme of the Instituto Geológico, Minero y Metalúrgico (INGEMMET, Peru). Also this institution financed the chemical and isotopic analysis of the samples. I warmly thank V. Carlotto for geological review and V. Vargas, Y. Antayhua and L. Cacya for fieldwork assistance. Aslo, I am grateful Phd María Aurora Armienta of the UNAM University for this Article Review.

References

Arnórsson, S., 1983. Chemical equilibria in Icelandic geothermal systems—implications for chemical geothermometry investigations. Geothermics 12, 119–128.

Arnórsson, S., 2000. Reactive and conservative components. En: Arnórsson, S., ed. Isotopic and chemical techniques in geothermal exploration, development and use: sampling methods, data handling, interpretation. Vienna: International Atomic Energy Agency, p. 40-48.

Aggarwal, J.K., Sheppard, D., Mezger, K., Pernicka, E., 2003. Precise and accurate determination of boron isotope ratios by multiple collector ICP-MS: origin of boron in the Ngawha geothermal system, New Zealand: Chemical Geology, v. 199, p. 331-342.

Arehart, G., Coolbaugh, M. F., Poulson, S. R., 2003. Evidence for a magmatic source of heat for the Steamboat Springs geothermal systems using trace elements and gas geochemistry: Geothermal Resources Council Transactions, v. 27, p. 269-274.

Baker, M., 1981. The nature and distribution of upper cenozoic ignimbrite centres in the Central Andes, Journal of Volcanology and Geothermal Research, 11, 293–315, 1981.

Barazangi, M. and Isacks, B.L., 1976. Spatial distribution of earthquakes and subduction of the Nazca plate beneath South America. Geology, 4: 686-692.

Babeyko, A., Sobolev, S., Trumbull, R., Oncken, O., Lavier, L., 2002. Numerical models of crustal scale convection and partial melting beneath the Altiplano - Puna plateau. Earth Planetary Sci. Letters, 199, 373–388.

Barazangi, W., Isacks, BL., 1976. Spatial distribution of earthquakes and subduction of the Nazca plate beneath South America. Geology 4:686–692.

Benavides, V., 1962. Estratigrafía Pre-terciaria de la región de Arequipa. En: Congreso Nacional de Geología, 2, Lima, 1960. Boletín Sociedad Geológica del Perú, (38):5-63.

Burgos, M. I.M., 1999. Geochemical interpretation of thermal fluid discharge from wells and springs in Berlín geothermal field, El Salvador. Report N° 7, Geothermal training programme, Reykjavík, Iceland, 165-191.

Chmielowsky, J., Zandt, G., Haberland, C., 1999. The Central Andean Altiplano Puna Magma Body, Geophys. Res. Lett., 26, 783–786.

Carlotto V.; Rodríguez, R.; Acosta, H.; Cárdenas, J., Jaillard, E., 2009. Alto estructural Totos-Paras (Ayacucho): límite paleogeográfico en la evolución mesozoica de las cuencas Pucará (Triásico Superior-Liásico) y Arequipa (Jurásico-Cretácico). Bol. Soc. Geol. Perú, 7, 1-46.

Cereceda, C.; Cerpa, L.; Muñoz, L.; Siesquen, D., Aguilar, R., 2012. Afinidad adakítica y sus implicancias en la evolución del magmatismo cenozoico y la tectónica en el sur del Perú. XVI Congreso Peruano de Geología, 5 p.

Clark, A.H.; Farrar, E.; Kontak, D.J.; Langridge, R.J.; Arenas, M., et al., 1990. Geologic and geochronologic constraints on the metallogenic evolution of the Andes of Southeastern Peru. Economic Geology, 85(7): 1520-1583.

Cruz, V., Vargas, V., Cacya, L., 2013. Caracterización y evaluación del potencial geotérmico de la región Tacna, INGEMMET, Bol. Serie C, 56, 165p (Lima, Perú).

Cruz, V., Vargas, V., Matsuda, K., 2010. Geochemical Characterization of Thermal Waters in the Calientes Geothermal Field, Tacna, South of Peru, Proceedings World Geothermal Congress, Bali, Indonesia (2010), paper 1454, 7pp.

Cruz, V., Vargas, V., Matsuda, K., 2010. Geochemical Characterization of Thermal Waters in the Borateras Geothermal Zone, Peru, Symp. On Water-Rock Interaction, I.A.G.C., Guanajuato, Mexico, 157-160.

Cortecci, G.; Boschetti, T.; Mussi, M.; Herrera, C.; Mucchino, C., Barbieri, M., 2005. New chemical and original isotopic data on waters from El Tatio geothermal field, northern Chile. Geochemical Journal, 39(6): 547-571.

Valdivia Cornejo Juan Gualberto (1874). Fragmentos para la historia de Arequipa. Folletín de "El Deber", Arequipa, 109-111 p.

De Silva, S., 1989. Altiplano-Puna volcanic complex of the central Andes, Geology, 17, 1102–1106,.

De Silva, V., Francis, P., 1991. Volcanoes of the Central Andes, Springer-Verlag, Berlin (216 pp).

Delacour, A., Gerbe, M.-C., Thouret, J.-C., Wörner, G., and Paquereau-Lebti, P., 2007. Magma evolution of Quaternary minor volcanic centres in southern Peru: Bulletin Bulletin of Volcanology, v. 69, p. 581–608, doi: 10.1007/s00445-006-0096-z.

De La Cruz, N. & De La Cruz, O. (2000) – Mapa geológico del Cuadrángulo de Tarata, escala 1: 50,000. Lima: Instituto Geológico Minero y Metalúrgico, 4 maps.

De La Cruz, N. & De La Cruz, O. (2001) - Memoria explicativa de la revisión geológica del cuadrángulo de Tarata (35-v), informe inédito. Lima. Instituto Geológico Minero y Metalúrgico, 19 p.

Díaz, G.; Montoya, A & Milla, D. (2000) - Mapa geológico del cuadrángulo de Maure, escala 1: 50,000. Lima: Instituto Geológico Minero y Metalúrgico, 4 maps.

Favara, R.O., Grassa, F., Inguaggiato, S., et al., 2001. Hydrogeochemistry and stable isotopes of thermal springs: earthquake-related chemical changes along Belice Fault (Western Sicily). Appl. Geochem. 16, 1–17.

Fouillac, C., Michard, G., 1981. Sodium/lithium ratio in water applied to geothermometry of geothermal reservoirs. Geothermics 10, 55-70.

Fournier, R.O., 1979. Geochemical and hydrologic considerations and the use of enthalpy-chloride diagrams in the prediction of underground conditions in hot spring system. Journal of Volcanology and Geothermal Research 5, 1-16.

Fournier, R.O., Potter, R. W., 1982. A revised and expanded silica (quartz) geothermometer. Geothermal Resource Council Bulletin 11, 3-9.

Giggenbach, W. F., 1984. Mass transfer in hydrothermal alteration systems. A conceptual approach, Geochim. Cosmochim. Acta, 48, 2693-2711.

Giggenbach, W. F., 1986. Graphical techniques for the evaluation of water/rock equilibrium conditions by use of Na, K, Mg, and Ca contents of discharge waters: Proceedings of Eighth New Zealand Geothermal Workshop, Auckland, New Zealand, p. 37-43.

Giggenbach, W.F., 1988. Geothermal solute equilibria; derivation of Na-K-Mg-Ca geoindicators. Geochimica et Cosmochimica Acta, 52(12): 2749-2765.

Giggenbach, W., 1989. The chemical and isotopic position of Ohaaki field within the Taupo Volcanic Zone. Proc. Eleventh N. Z. Geothermal Workshop, Aukland: 81-88.

Giggenbach, W.F., Gougel, R. L., 1989. Method for the collection and analysis of geothermal and volcanic water and gas samples. NZ-DSIR Report, CD 2387,53.

Giggenbach, W. F., 1991a. Chemical techniques in geothermal exploration. In: D'Amore, F. (Ed.): Application of Geochemistry in Geothermal

Reservoir Development (Coordinator D' Amore, F.). UNITAR/UNDP Center on Small Energy Resources, Rome, pp. 119-144.

Giggenbach, W.F., 1992. Chemical techniques in geothermal exploration. In D'Amore, F. (ed): Applications of Geochemistry in Geothermal Reservoir Development, UNITAR/UNDP, Rome.

Giggenbach, W.F., Sheppard, D.S., Robinson, B.W., Stewart, M.K., Lyon, G.L., 1994. Geochemical structure and position of the Waiotapu geothermal field, New Zealand. Geothermics 23 (5/6), 599–644.

Joseph E P, Fournier N, Lindsay J M, Robertson R and Beckles D M (2013) Chemical and isotopic characteristics of geothermal fluids from Sulphur Springs, Saint Lucia, Journal of Volcanology and Geothermal Research, 254, 23-36.

Jordan, T., Isacks, B., Allmendinger, R., Brewer, J., Ramos, V., Ando, C., 1983. Andean Tectonics related to geometry of subducted Nazca plate, Geol. Soc. Am. Bull. 94, 341-361.

Kono, M., Fukao, Y., Yamamoto, A., 1989. Mountain Building in the Central Andes, J. Geophysical Res., 94, 3891-3905.

Keenan, J.H., Keyes, F.G., Hill, P.G., Moore, J.G., 1969. Steam Tables – Thermodynamic Properties of Water Including Vapour, Liquid and Solid Phases (international edition – metric units). Wiley, New York, pp. 162.

Lahsen, A., 1982. Upper Cenozoic volcanism and tectonism in the Andes of Northern Chile, Earth Science Reviews, 18, 285–302.

Martini, M., Giannini, L., Prati, F., Tassi, F., Capaccioni, B., andIoizzelli, P., 1994. Chemical characters of crater lakes in the Azores and Italy: the anomaly of Lake Albano, Geochem. J., 28, 173–184.

Manrique N., 2013). Evolución Vulcanológica y Magmática del Edificio Reciente del Complejo Volcánico Tutupaca (Tacna). Universidad Nacional San Agustín de Arequipa. Tesis. 90 p.

Mutlu, H., 1998. Chemical geothermometry and fluid–mineral equilibria for the Ömer-Gecek thermal waters, Afyon area, Turkey, J. Volcanol. Geotherm. Res., vol. 80, p.303-321.

Nicholson, K. (1993) - Geothermal fluids: Chemistry and exploration techniques. Berlin: Springer-Verlag, 278 p.

Nieva, D., Nieva, R., 1987. Developments in geothermal energy in Mexico, part 12—A cationic composition geothermometer for prospection of geothermal resources. Heat recovery systems and CHP 7, 243–258.

Ramos, V.A.; Alemán, A. 2000. Tectonic Evolution of the Andes. In Tectonic evolution of South America (Cordani, U.G.; Milani,

E.J.; Thomaz Filho, A.; Campos, D.A.; editors). International Geological Congress, No. 31, p. 635-685. Río de Janeiro.

Riogilang, H., Itoi, R., Taguchi, S., 2013. Conceptual model hydrothermal system at Kotamobagu geothermal field, nort Sulawesi, Indonesia, Procedia Earth and Planetary Science 6, 83-90.

Sepúlveda, F. et al., 2004. Chemical and isotopic composition of geothermal discharges from the Puyehue-Cordón Caulle area (40.5°S), Southern Chile. Geothermics, Vol. 33(5), 655–673 p.

Siebert L, Simkin T, Kimberly P (2010) Volcanoes of the world. Third edition. Smithsonian Institution and University of California press. 551 p

Steinmüller, K., Zavala, B., 1997. Hidrotermalismo en el Sur del Perú. INGEMMET, Boletín, Serie D: Estudios Regionales, 18, 79 p.

Stauder, W., 1975. Subduction of the Nazca plate under Peru as evidenced by focal mechanisms and by seismicity. Journal of Geophysical Research 80: doi: 10.1029/JB080i008p01053. issn: 0148-0227.

Shigeno, H. & Abe, K. (1983) - B-C1 geochemistry applied to geothermal fluids in Japan, especially as an indicator for deep-rooted hydrothermal systems. En: International Symposium on Water-Rock Interaction, 4, Misasa, 1983. Extended abstracts. International Association of Geochemistry, p. 437-440.

Shigeno, H.; Takahashi, M & Noda, T. (1993) - Reservoir environment of the Onuma geotermal power plant, northeast Japan, estimated by forward analysis of long-term artificial tracer concentration change, using single-box-model simulator. En: Workshop on Geothermal Reservoir Engineering, 18, California, 1993. Proceedings. California: Stanford University, p. 135-140.

Tassi, F., Aguilera, F., Darrah, T., Vasseli, O., Capaccioni, B., Poreda, R.J., Huertas, A.D., 2010. Fluid geochemistry of hydrothermal systems in the Arica-Parinacota, Tarapace and Antofagasta regions (northern Chile). Journal of Volcanology and Geothermal Research 192, 1–15.

Taran Yu.A., Pokrovsky B. G., and Esikow A. D., 1989. Deuterium and oxygen-18 in fumarolic steam and amphiboles from some Kamchatka volcanoes: "andesitic waters." Dokl. Akad. Nauk. USSR 340, 440–443.

Truesdell, A.H., Fournier, R.O., 1977. Procedure for estimating the temperature of a hot water component in a mixed water using a plot of dissolved silica vs. enthalpy. Journal of Research of the U.S. Geological Survey 5, 49–52.

Tonani, F., 1980. Some remarks on the application of geochemical techniques in geothermal exploration. Proc. Adv. Eur. Geoth. Research, 2nd Symposium, Strasbourg, pp. 428–443.

Torres, V.; Gonzalez, E.; Barragán, R.; Birkle, P.; Nieva, D., et al. (1997) - Estudio de prefactibilidad del proyecto geotérmico Tutupaca, Perú, informe inédito. Morelia (México): Instituto de Investigaciones Eléctricas, 76 p.

Truesdell, A.H., 1976. Summary of Section III: Geochemical techniques in exploration, Proceedings of the Second United Nations Symposium on the Development and Use of Geothermal Resources. San Francisco, CA, USA, 20-29 May, 1975, Vol. 1.

Valley, J., Taylor, H., ONeil, J., 1986. Stable isotopes. Reviews in Mineralogy, 16. Mineralogical Society of America.

Vargas, V., Cruz, V., Cacya, L., 2012. Caracterización y evaluación del potencial geotérmico de la región Tacna, INGEMMET, Bol. Serie C, 56, 165p (Lima, Perú).

Vargas, V., Cruz, V., 2010. Geothermal map of Perú, Proceedings World Geothermal Congress, Bali, Indonesia (2010), paper 1627, 5pp.

Valdivia JG., 1847. Fragmentos para la historia de Arequipa. Folletín de "El Deber", Arequipa, 109–111 p

Vicente, J.C., Sequeiros, F.; Valdivia, M., Zavala, J., 1979. El sobre-escurrimiento de Cincha-Lluta: elemento del accidente mayor andino al NW de Arequipa. Boletín Sociedad Geológica del Perú, (61): 67-99.

West Japan Engineering Consultants, 2012. The master plan for development of geothermal energy in Peru, final report. [s.l.]: Japan International Cooperation Agency and West Japan Engineering Consultants, 138 p.

Zamácola y Jaúregui JD., 1804. Apuntes para la historia de Arequipa. Imp. De La Bolsa-Guañamarca, N. 49. 1888.